Exchange Anisotropy in Nanocasted Co3O4 Nanowires

ARTICLE *in* NANO LETTERS · AUGUST 2006

Impact Factor: 13.59 · DOI: 10.1021/nl060528n

NANO LETTERS

2006
Vol. 6, No. 12
2977−2981

Exchange Anisotropy in Nanocasted Co_3O_4 Nanowires

Elena Lorena Salabaş,*,† Anja Rumplecker,† Freddy Kleitz,‡ Florin Radu,§ and Ferdi Schüth†

Max-Planck-Institut für Kohlenforschung, Kaiser-Wilhelm-Platz 1, D-45470 Mülheim an der Ruhr, Germany, Department of Chemistry, Université Laval, St Foy, G1K7P4, Québec, Canada, and BESSY GmbH, Albert-Einstein Strasse 15, D-12489, Berlin, Germany

Received March 8, 2006; Revised Manuscript Received August 19, 2006

ABSTRACT

Antiferromagnetic Co_3O_4 nanowires with an average diameter of about 8 nm have been synthesized by using the nanocasting route. The nanowires were characterized by powder X-ray diffraction, transmission electron microscopy, and a superconducting quantum interference device magnetometer. The magnetic measurements show a unidirectional exchange anisotropy accompanied by an enhancement of the field-cooled coercivity at low temperature. These effects suggest the presence of an exchange interaction between the antiferromagnetic core and the surface spins. A strong dependence of the exchange field on the magnitude of the cooling field and a training effect have been observed. The dependence of exchange bias field on temperature reveals the important role played by the antiferromagnetic core in the exchange coupling.

Magnetism of antiferromagnetic nanoparticles provides a particularly interesting case due to their potential for exhibiting magnetization reversal by quantum tunneling,[1] their weak ferromagnetism below the Néel temperature,[2,3] as well as for their applications in spin-valve systems.[4] The breaking of the large number of exchange bonds of the surface atoms, a large surface/volume ratio, the surface roughness, and the breaking of the symmetry are only a few of the underlying causes that can change considerably the magnetic properties of small particles.[6] In particular, for small particles with an antiferromagnetically ordered core, the surface spins are expected to dominate the magnetic properties. In this letter, we present results on nanocast antiferromagnetic Co_3O_4 nanowires.

Recently, significant progress has been achieved in the preparation of nanostructured materials by utilizing the so-called *nanocasting* route.[7,8] According to this method, an ordered porous carbon or silica matrix acts as a nanoscopic mold, which restricts, through confinement, the formation and growth of metal or metal oxide species.[9,10] Various nanoobjects such as nanoparticles, nanowires, or nanostructured networks can form selectively in the voids of porous silica. Especially interesting with respect to magnetic properties are nanocasted Co_3O_4 samples.[10,11]

The nanocasted Co_3O_4 nanowires were prepared by employing hexagonally ordered mesoporous SBA-15 silica as a hard template. The SBA-15 material was obtained using the conditions proposed by Choi et al.[12] Mesoporous SBA-15 was prepared at low HCl concentration (0.3 M) in aqueous solution using tetraethoxysilane (TEOS, Acros 99%) as a silicon source and Pluronic P123 ($EO_{20}PO_{70}EO_{20}$, Sigma-Aldrich) as the structure-directing agent. After calcination at 823 K, the structure of mesoporous SBA-15 silica was confirmed by powder X-ray diffraction (PXRD) and nitrogen physisorption at 77 K (data not shown). The SBA-15 had a surface area of 857 $m^2\ g^{-1}$, a pore volume of 1.15 $cm^3\ g^{-1}$, and an average pore size of 8 nm. The pore size was calculated from the adsorption branch using the Barrett−Joyner−Halenda (BHJ) algorithm. In the next step, 0.2 g of SBA-15 was dispersed in 2 mL of a 0.8 M solution of $Co(NO_3)_2 \cdot 6\ H_2O$ (Fluka 99%) in ethanol and stirred at 298 K for 1 h. At this stage, because of capillary effects, the pores are filled with the precursor solution. After drying at 353 K, the resulting pink powder was heated at 473 K for 10 h. The impregnation and decomposition step was repeated once following the same conditions. The resulting material was then calcined at 723 K for 6 h. The silica template was removed using a 2 M NaOH aqueous solution at 300 K. The Co_3O_4 material was recovered by centrifugation, washed with water, and finally dried at 323 K. The formation process of Co_3O_4 nanowires in the Co_3O_4/silica composite was followed with nitrogen physisorption (data not shown), transmission

* Corresponding author. E-mail: salabas@mpi-muelheim.mpg.de.
† Max-Planck-Institut für Kohlenforschung.
‡ Department of Chemistry, Université Laval.
§ BESSY GmbH.

10.1021/nl060528n CCC: $33.50
Published on Web 11/01/2006

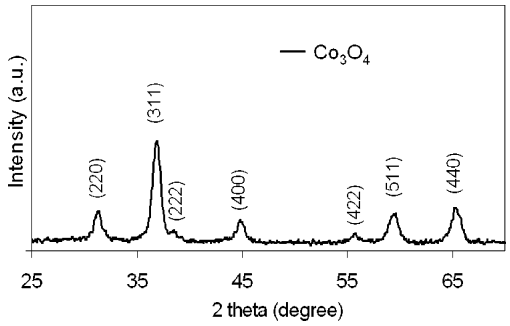

Figure 1. Wide-angle XRD pattern of Co_3O_4.

electron microscopy (TEM), and wide-angle powder X-ray diffraction (XRD).

In Figure 1, the wide-angle powder X-ray diffraction pattern of Co_3O_4 is shown. The diffraction peaks identify the sample as pure spinel Co_3O_4. No indication of cobalt silicates were observed in XRD analysis. The nanocasted Co_3O_4 have large surface areas of 122 $m^2\ g^{-1}$ and exhibit single crystallinity in domains. Energy dispersive X-ray (EDX) analysis proved the removal of silica down to trace levels (<1%). Transmission electron microscopy images (Figure 2) reveal that the sample mostly consists of randomly organized arrays of Co_3O_4 nanowires. The average diameter of the nanowires as observed by TEM is 8 nm, reflecting the pore size of the parent silica matrix. The length of the nanowires is up to 100 nm.

The magnetic characterization of the samples was performed by using a superconducting quantum interference device (SQUID) magnetometer. The magnetic measurements have been done on various Co_3O_4 samples with fully reproducible results. The magnetic response is determined by a complex interplay between the intrinsic properties of one nanoparticle itself and the collective magnetic properties. Any effect on the magnetic properties caused by the shape anisotropy of the nanowires will not be resolved in our experiments because the measurements were done on powders with randomly oriented Co_3O_4 nanowires. The results of zero-field-cooled (ZFC) and field-cooled (FC) temperature-dependent measurements performed on Co_3O_4 nanowires are shown in Figure 3. In ZFC measurement, the sample is cooled from room temperature to 3 K without applying an external magnetic field. After reaching $T = 3$ K, the magnetization is recorded on warming and in a weak external field of 50 Oe. For the FC experiment, the sample is cooled from room temperature in an applied magnetic field of 40 kOe. Subsequently, the sample magnetization is recorded in an external magnetic field of 50 Oe as temperature is increased. The ZFC curve exhibits a broad peak around 30 K (see the inset of Figure 3), which corresponds to the Néel transition. At low temperatures, the FC magnetization rapidly increases with decreasing temperature, becoming five times larger than the ZFC magnetization at $T = 3$ K. This low temperature behavior of the FC magnetization curve can be attributed to the surface spins, which are frozen in the external field direction. At higher temperatures, when the particle moments are free to thermal fluctuations, the ZFC and FC curves merge together.

The magnetization dependence on the applied magnetic field (hysteresis loops) recorded at $T = 2$ K under zero-field-cooled (ZFC) conditions is shown in Figure 4a. The hysteresis loop recorded after cooling the system in zero external field exhibits a small hysteresis (with a remanent magnetization of 0.02 emu/g), which is symmetrical and

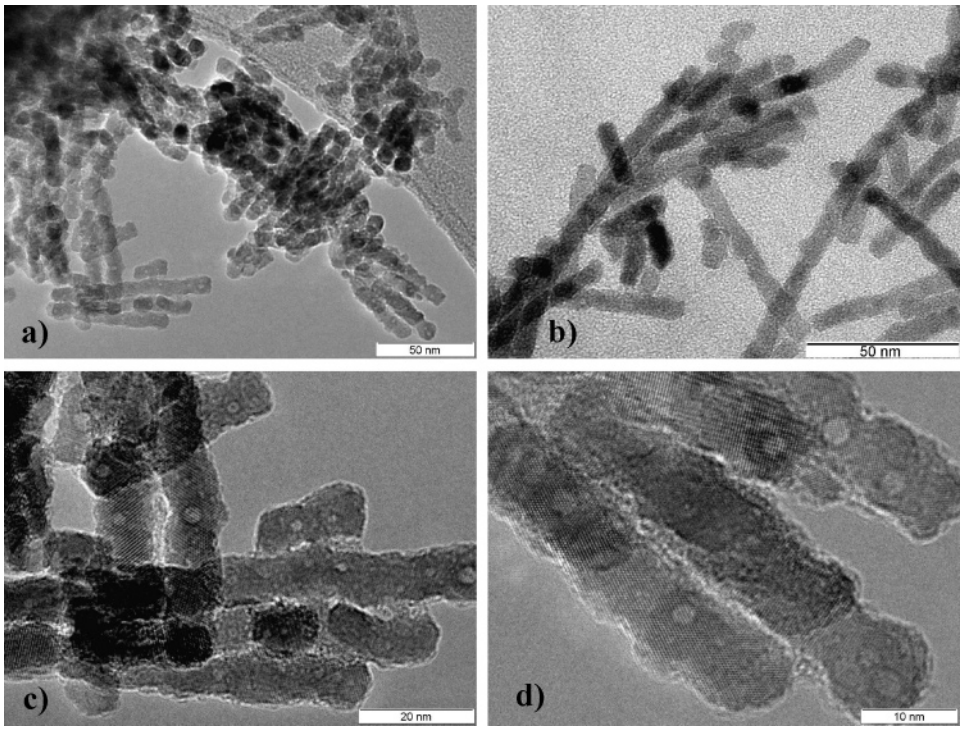

Figure 2. Different magnifications TEM images of the Co_3O_4 nanowires.

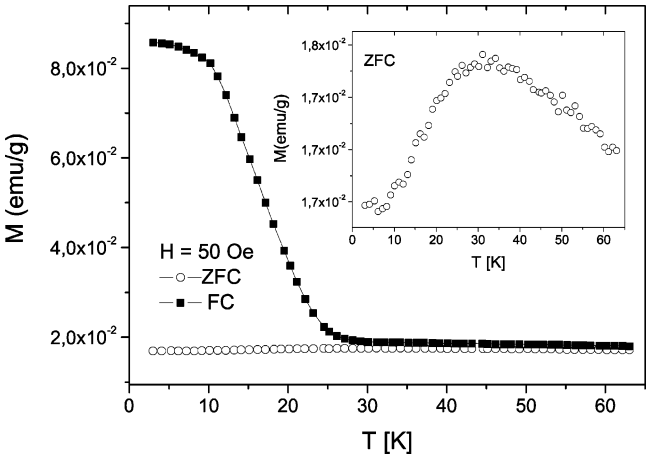

Figure 3. Zero-field-cooled (open circles) and field-cooled (full squares) magnetization curves measured in an applied magnetic field of 50 Oe as a function of temperature. The cooling field was 40 kOe. The inset displays an extended part of ZFC curve.

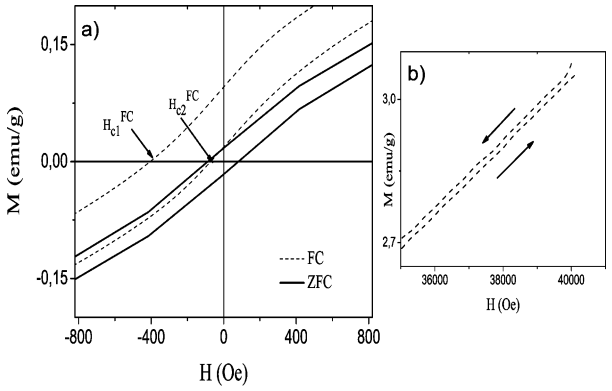

Figure 4. (a) Central part of ZFC (solid lines) and FC (dashed lines) hysteresis loops measured at $T = 2$ K. (b) High-field irreversibility of magnetization on the right-hand side. On the left-hand side, the hysteresis loop is closed (data not shown).

centered about the origin. A coercive field of $H_c^{ZFC} = 82 \pm 10$ Oe was measured. The origin of this weak ferromagnetism at low temperature is due to the small dimensions of the particles because, for a bulk antiferromagnet, the sublattice magnetizations are fully compensated, resulting in zero net magnetization. Similar behavior for a system of antiferromagnetic nanoparticles has been reported for NiO,[2] α-Fe_2O_3[13], and a cubic Co_3O_4 mesostructure.[10] Different models have been proposed to explain this weak ferromagnetism in small antiferromagnetic nanoparticles. For example, Néel[14] attributed this to the uncompensated spins on two sublattices. Kodama et al.[2] have proposed a model where the spins in antiferromagnetic nanoparticles yield multisublattice configuration, indicating that the reduced coordination of surface spins leads to an important change in the magnetic order of the whole particle. The presence of some external magnetic impurities in our sample has been ruled out by means of X-ray photoelectron spectroscopy (XPS) analysis, where no traces of metallic cobalt have been detected. No other magnetic impurities have been identified by EDX analysis, either.

To gain further insight into the origin of this small net magnetization of Co_3O_4 nanowires, field-cooled hysteresis loop have been recorded (Figure 4a). The FC hysteresis loops were measured after cooling the sample in an applied field of 40 kOe through the Néel temperature. Remarkably, the FC magnetization curve exhibits the typical features of an exchange bias system, namely a shift of the hysteresis loop toward negative magnetic fields and enhanced coercivity. In addition, a shift upward of the hysteresis loop ($M_{shift} = |M(H_+)| - |M(H_-)|$), a training effect accompanied by open loops up to 40 kOe, and a tunable magnitude of the exchange field via cooling field are directly observed. All these noticeable findings will be discussed below.

Usually, the horizontal shift of the hysteresis loop occurs when a ferromagnet (FM) is in contact with an antiferromagnet (AFM) and the entire system is cooled through the Néel temperature of the antiferromagnet.[4,5,15] The exchange coupling present at the interface between the FM and the AFM induces a unidirectional anisotropy of the ferromagnetic layer. The strength of the unidirectional anisotropy is measured by the exchange bias field $H_{eb} = (H_{c2}^{FC} + H_{c2}^{FC})/2$. A value of $H_{eb} = -240$ Oe at $T = 2$ K has been measured for the Co_3O_4 nanowires sample. H_{c1}^{FC} and H_{c2}^{FC} are marked in Figure 4a. The error bar in the determination of the exchange bias values is less than 10%. An additional confirmation of the presence of AFM−FM coupling giving rise to the unidirectional anisotropy is the enhancement (two times larger) of the coercive field after field cooling. The appearance of horizontally shifted hysteresis loops in the Co_3O_4 nanowires suggests the existence of an exchange coupling between the AFM core spins and the FM-like surface spins. As a result of low coordination and broken symmetry, the surface spins have different anisotropy compared to the core spins and may be considered to behave like a spin-glass-like system (frustrated system) with multiple stable spin configurations.[19] We assume that, because of the reduced anisotropy at the interface, the surface spins contribute to the total magnetization in two ways: one part consists of frozen-in uncompensated spins, which do not reverse during the field cycling. They are the spinning, uncompensated "interfacial" spins necessary for the exchange bias to exist.[15,18] In the hysteresis loop, they are visible as a shift upward along the magnetization axis of about 0.07 emu/g; the other part of the AFM surface spins behave similarly to ferromagnetic spins, and they can be aligned by the external field. These two components, observed directly in the hysteresis loop, can be understood as being caused by a variation of the anisotropy from the bulk value toward low values at the location of the outer spins.[16] A sharp change of the AFM anisotropy at a presumably ideal interface between a monodomain AFM and the FM layer would cause no enhanced coercivity. In contrast, a rather slow variation of the anisotropy of the AFM surface spins provides the qualitative understanding for both frozen and reversible spins responsible for the upward shift of the hysteresis loop and enhanced coercivity, respectively.

The spin-glass (SG) like behavior of the surface spins is clearly seen as an open hysteresis loop in the upper right

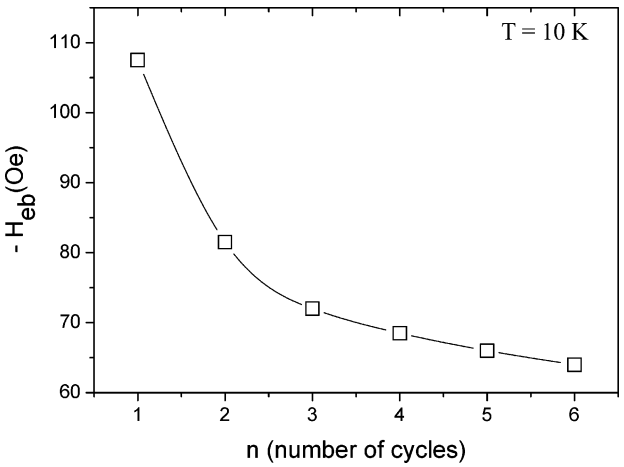

Figure 5. Field cycle dependence of the exchange bias field recorded at $T = 10$ K.

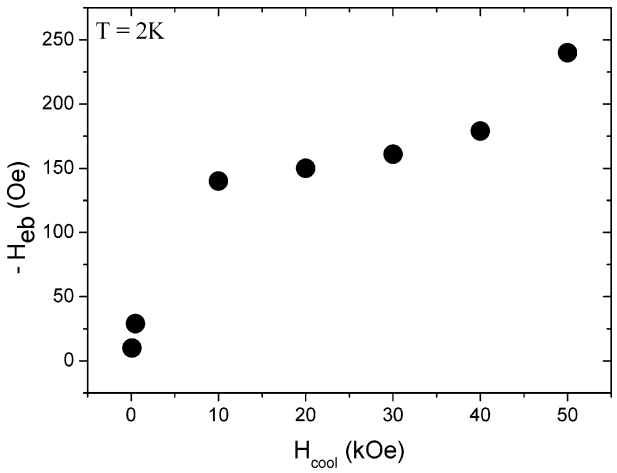

Figure 6. Exchange bias field as a function of cooling field measured at $T = 2$ K.

side of the FC hysteresis loop, which is shown in Figure 4b. This indicates that we have a loss of magnetization during one hysteresis cycle. This striking experimental feature is observed here because of the large amount of measured material (21 mg of powder) and due to the absence of additional ferromagnetic materials, which could mask the observation of the "interfacial" spins behavior. In thin films, such an effect is predicted to be about 5% of the magnetization of an AFM uncompensated monolayer (see Figure 4 of ref 17). This value lies below the sensitivity of laboratory methods like SQUID. Therefore, such an effect can be hardly observed experimentally in thin films, but only in a system as studied here. Moreover, a reduction of the exchange bias field upon subsequent magnetization loops has been measured. This gradual decrease of the exchange field with the number of cycles is called training effect and is shown in Figure 5. To study the training effect, the system was cooled in 50 kOe from room temperature to 10 K and six complete hysteresis loops were recorded. A significant reduction of the exchange bias was measured between the first and the second loops where H_{eb} falls by ~25%. This training effect can be associated with an instability of the spin structure, which leads to a reduction of magnetization after repetitive hysteresis cycles. Both effects (open loops and training effect) support the assumption of a spin-glass-like surface with multiple spin configuration, when a rearrangement of the surface spins is present after each magnetization reversal. It becomes clear that, in an exchange-bias system, the progressive increase of the interface disorder is related to a loss of frozen-in magnetization, which further leads to an open hysteresis loop. Besides that, a strong dependence of the cooling field on the exchange bias magnitude is another fingerprint for the existence of a spin-glass-like phase at the surface. Figure 6 shows the influence of the cooling field on the magnitude of the exchange field. We have observed that the exchange bias increases with increasing cooling field. This can be explained as follows: by increasing the magnitude of the cooling field, more uncompensated spins are aligned with the magnetic field and rotate. These spins will lead to changes in the magnetic configuration at the surface and implicitly at the AFM core/FM shell interface.

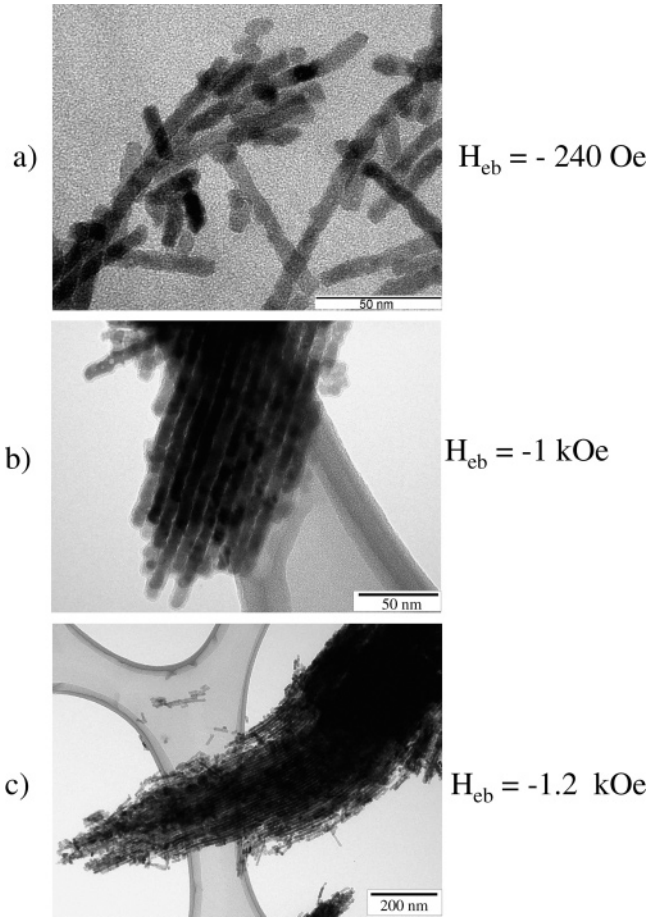

Figure 7. TEM images of nanocasted Co_3O_4 with different loadings: (a) 15%, (b) 18%, (c) 24%. The exchange field yields a systematic change as a function of the nanowires surface disorder.

Thus, with increasing the magnitude of the cooling field, more and more frozen-in spins are created and a tunable exchange bias field is obtained.

Interestingly, we have observed that, by varying the degrees of order of the mesoporous nanowires, the magnitude of the exchange bias field can be modified. By a careful selection of the network interconnectivities of the parent silica and the loading parameter, the structure could be tune from

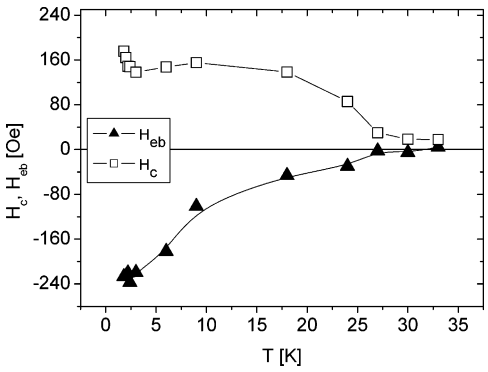

Figure 8. Temperature dependence of the exchange bias field (triangles) and FC coercivity (squares). The lines are guides to the eye.

isolated or randomly organized Co_3O_4 nanowires to fully interconnected, highly ordered mesoporous nanowires. More details about nanocasting of different Co_3O_4 nanostructures are given in ref 20. In Figure 7, the TEM images of three different samples with different degrees of order are shown. The loading values are given as volume percent of the accessible pore volume filled with Co_3O_4. Figure 7 clearly shows that the magnitude of the exchange bias increased for the samples with high interconnectivity. An increase of loading parameter from 15% to 24% results in 6 times larger value of the exchange bias field. The data clearly shows that the exchange bias field systematically changes as a function of the nanowires surface disorder.

The exchange bias field and FC coercivity as a function of temperature are shown in Figure 8. The samples were cooled from above the Néel temperature to the respective target temperatures below T_N in a magnetic field of 40 kOe. The exchange bias field decreases with increasing temperature and completely vanishes slightly below the Néel temperature. Above the Néel temperature, the AFM spins are in a paramagnetic state and, therefore, are unable to bias the ferromagnetic spins and to give rise to coercivity. The FC coercivity diminishes when the Néel temperature is approached.

In summary, highly crystalline Co_3O_4 nanowires have been prepared via the nanocasting route in the hexagonally ordered array of mesopore SBA-15. The results indicate that the magnetic behavior of the Co_3O_4 nanowires is mainly determined by surface effects, with the surface spins behaving similar to a spin-glass-like system. An exchange anisotropy followed by an enhancement of the coercivity has been measured. An opening of hysteresis loop related to the training effect is clearly observed. The magnitude of the exchange bias field can be tuned by the strength of the cooling field and the interconnectivity between Co_3O_4 nanowires. The exchange bias field sets slightly below the Néel temperature. This indicates that exchange bias vanishes once the order of the AFM core is lost, emphasizing the crucial role played by the AFM layer in the observed exchange bias interaction.

Acknowledgment. We thank Dr. C. Weidenthaler for the XPS measurements and A. Göbels (Max-Planck Institute for Bioinorganic Chemistry, Mülheim, Germany) for the SQUID measurements. Thanks are due to B. Spliethoff for the HRTEM images. This work was supported partially by the Leibniz Program of the DFG.

References

(1) Friedman, A. J. R.; Voskoboynik, U.; Sarachik, M. P. *Phys. Rev. B* **1997**, *56*, 10793.
(2) Kodama, R. H.; Makhlouf, S. A.; Berkowitz, A. E. *Phys. Rev. Lett.* **1997**, *79*, 1393.
(3) Makhlouf, S. A. *J. Magn. Magn. Mater.* **2002**, *246*, 184.
(4) Nogués, J.; Schuller, I. K. *J. Magn. Magn. Mater.* **1999**, *192*, 203.
(5) Nogués, J.; Sort, J.; Langlais, V.; Skumryev, V.; Suriñach, S.; Muñoz, J. S.; Baró, M. D. *Phys. Rep.* **2005**, *422*, 65.
(6) Kodama, R. H.; Berkowitz, A. E. *Phys. Rev. B* **1999**, *59*, 6321.
(7) Schüth, F. *Angew. Chem., Int. Ed.* **2003**, *42*, 3604.
(8) Yang, H.; Zhao, D. *J. Mater. Chem.* **2005**, *15*, 1217.
(9) Shin, H. J.; Ko, C. H;. Ryoo, R. *J. Mater. Chem.* **2001**, *11*, 260.
(10) Wang, Y.; Yang, C. M.; Schmidt, W.; Spliethoff, B.; Bill, E.; Schüth, F. *Adv. Mater.* **2005**, *17*, 53.
(11) Tian, B.; Liu, X.; Yang, H.; Xie, S.; Yu, C.; Tu B.; Zhao, D. *Adv. Mater.* **2003**, *15*, 1370.
(12) Choi, M.; Heo, W.; Kleitz, F.; Ryoo, R. *Chem. Commun.* **2003**, *12*, 1340.
(13) Zysler, R.; Fiorani, D.; Dormann, J. L.; Testa, A. M. *J. Magn. Magn. Mater.* **1994**, *133*, 71.
(14) Neel, L. *Low Temperature Physics*; DeWitt, Dreyfus, B. de Gennes, P. D., Eds.; Gordon and Breach: New York, 1962.
(15) Meiklejohn, W. H.; Bean, C. P. *Phys. Rev.* **1956**, *102*, 1413.
(16) Radu, F.; Westphalen, A.; Theis-Bröhl, K.; Zabel, H. *J. Phys.: Condens. Matter* **2006**, *18*, L29−L36.
(17) Nowak, U.; Usadel, K. D.; Keller, J.; Miltényi, P.; Beschoten, B.; Güntherodt, G. *Phys. Rev. B* **2002**, *66*, 014430.
(18) Ohldag, H.; Scholl, A.; Nolting, F.; Arenholz, E.; Maat, S.; Young, A. T.; Carey, M.; Stöhr, J. *Phys. Rev. Lett.* **2003**, *91*, 017203.
(19) Gruyters, M. *Phys. Rev. Lett.* **2005**, *95*, 077204.
(20) Rumplecker, A.; Kleitz, F.; Salabas, E. L.; Schüth, F. *Chem. Mater.* **2006**, in revision.

NL060528N